In Vitro Cellular & Developmental Biology - Animal
https://doi.org/10.1007/s11626-024-00970-8

Inhibition of FOXO3 ameliorates ropivacaine-induced nerve cell damage through the miR-126-5p/TRAF6 axis

Song Peng[1] · Yuzeng Xu[2] · Xiao Lin[3]

Received: 13 May 2024 / Accepted: 15 August 2024 / Editor: Tetsuji Okamoto

Abstract
Local anesthetics, such as ropivacaine (Ropi), are toxic to nerve cells. We aimed to explore the role of forkhead box O3 (FOXO3) in Ropi-induced nerve injury to provide a theoretical basis for reducing the anesthetic neurotoxicity. SK-N-SH cells were cultured and treated with different concentrations of Ropi. Cell viability, apoptosis, cytotoxicity (LDH/ROS/SOD), and levels of FOXO3, miR-126-5p, and tumor necrosis factor receptor–associated factor 6 (TRAF6) were detected. The enrichment of FOXO3 on the miR-126-5p promoter was analyzed. The binding relationships among FOXO3, miR-126-5p promoter sequence, and TRAF6 3′UTR sequence were verified. Combined experiments detected the regulatory role of FOXO3/miR-126-5p/TRAF6 in Ropi-induced nerve injury. FOXO3 was upregulated in Ropi-induced nerve cell damage. Inhibition of FOXO3 ameliorated Ropi-induced decreased cell viability, and increased apoptosis and cytotoxicity. FOXO3 bound to the miR-126-5p promoter and inhibited its expression, thereby counteracting miR-126-5p-induced repression. miR-126-5p inhibition and TRAF6 overexpression partially reversed the alleviative effect of FOXO3 inhibition on Ropi-induced nerve cell damage. In conclusion, FOXO3 aggravated the neurotoxicity of Ropi through miR-126-5p downregulation and TRAF6 upregulation, suggesting that FOXO3 inhibitor could be an adjuvant agent for local anesthetics, to alleviate local anesthetics-induced neurotoxicity.

Keywords Ropivacaine · Nerve injury · FOXO3 · MiR-126-5p · TRAF6

Introduction

Local anesthetics (LAs) are the only drugs that can completely block the noxious impulse from reaching the cerebral cortex (Barletta and Reed 2019). Despite the anesthetic benefits, LAs including bupivacaine, levobupivacaine, and ropivacaine (Ropi), which can cause neurotoxicity and cardiotoxicity in a plasma concentration-dependent manner (Barletta and Reed 2019). Ropi is one of the LAs with neurotoxic potential, inducing thermal hyperalgesia and mechanical allodynia, as well as neuronal damage (Hampl *et al*. 2014). Although Ropi is comparatively less toxic to the central nervous system, it may still trigger neurotoxicity manifested as neuronal pyroptosis/apoptosis, elevated lactate dehydrogenase (LDH), and mitochondrial dysfunction (Chen *et al*. 2019; Xu *et al*. 2022; Zhang and Wang 2023). Therefore, it is necessary to explore the mechanism of Ropi-induced nerve injury so as to provide a theoretical basis for reducing the neurotoxicity caused by local anesthetics.

Forkhead box O (FOXO) proteins are evolutionarily conserved transcription factors that play a role in regulating neural cell survival, stress response, lineage commitment, and neuronal signaling (Santo and Paik 2018). FOXO3 is involved in biological processes, such as inflammation, metabolism, cell death, and aging (Cao *et al*. 2023). Previous studies have shown that FOXO3 is involved in many neurological diseases. For instance, FOXO3 is involved in Mn-induced neuroinflammation (Yan *et al*. 2023); silencing FOXO3 alleviates brain injury after intracerebral hemorrhage and inhibits neuronal ferroptosis (Qin *et al*. 2022). More importantly, knockdown of FOXO3 can block neuronal autophagy and improve brain edema and neurological

✉ Xiao Lin
linxiao9898@163.com

[1] Department of Anesthesiology, Affiliated Xiaoshan Hospital, Hangzhou Normal University, Hangzhou, China

[2] Department of Anesthesiology, Affiliated Xiaoshan Hospital, Hangzhou Normal University, Hangzhou, China

[3] Department of Anesthesiology, Women's Hospital School of Medicine Zhejiang University, 1 Bachelor Road, Hangzhou 310006, Zhejiang, China

Published online: 03 September 2024

deficits after brain injury (Bhargava *et al*. 2017). Inhibition of FOXO3 expression has neuroprotective effects on neural stem cells, which can protect neural stem cells from sevoflurane-induced abnormal differentiation (Zeng *et al*. 2022). However, the role of FOXO3 in Ropi-induced nerve injury has not been reported.

MicroRNAs (miRNAs) are genetic regulators that can regulate physiological processes and pathologies by interacting with a wide range of target genes through recognition of 3′-untranslated regions (Diener *et al*. 2022). Previous studies showed that miRNAs are involved in anesthetic-induced nerve injury; for example, miRNA-384-3p can reduce sevoflurane-induced neurotoxicity (Chen *et al*. 2022); knockdown of miR-206 can increase the level of brain-derived neurotrophic factor, thereby alleviating the ketamine-induced nerve injury (Yao *et al*. 2020). More importantly, miR-126-5p is involved in the regulation of stroke (Pan *et al*. 2020) and Parkinson's disease (Mao *et al*. 2023). It has been reported that downregulation of miR-126 exacerbates neuronal death after cerebral ischemia–reperfusion (Xiao *et al*. 2020). In addition, FOXO3 has been demonstrated to finetune the expression of miRNAs, such as miR-34b/c and miR-21 (Wu *et al*. 2021). However, there is no report on the role of FOXO3/miR-126-5p in local anesthesia-induced neurotoxicity.

TRAF is a key signaling molecule for transducing signals and plays an important role in immune response, cell death and survival, cell development, and thrombosis (Park 2018). TRAF6 acting as an adaptor of a neurotrophin receptor promotes nerve growth factor survival (Roux and Barker 2002) and inhibition of TRAF6 in astrocytes can alleviate neuropathic pain (Lu *et al*. 2015). TRAF6 is a key factor in the incidence of cerebral ischemia (Wu *et al*. 2013). Knockdown of TRAF6 alleviates ferroptosis, inflammation, and cognitive dysfunction in mice with Alzheimer's disease (Ye *et al*. 2023). Overexpression of TRAF6 promotes the activation of NF-κB, thereby reducing the toxic effects on neurons (Chen and Zhuang 2023). Through the database, we predicted that TRAF6 was located downstream of miR-126-5p. In this study, the mechanism of FOXO3 in Ropi-induced nerve injury was explored to provide a theoretical basis for the treatment of neurotoxicity caused by LAs.

Materials and methods

Cell culture In alignment with preceding studies (Xue *et al*. 2020; Wang *et al*. 2023), our investigation employed Ropi for local anesthesia. The human neuroblastoma cell lineage SK-N-SH was obtained from ATCC (Manassas, VA). The cell culture was conducted in Dulbecco's modified Eagle's medium (DMEM, Gibco, Grand Island, NY) containing 10% fetal calf serum, 100 IU/mL penicillin G sodium, and 100 mg/mL streptomycin sulfate and was preserved in an incubator at 37℃ with 5% CO_2. The cells were identified using short tandem repeat and confirmed to be negative for *Mycoplasma* infection using the *Mycoplasma* detection kit (MP0035, Sigma, St. Louis, MO).

Cell treatment Ropi (MedChemExpress, Monmouth Junction, NJ) was diluted with 0.9% saline prepared by ddH_2O. The treatment of SK-N-SH cells was performed using different concentrations of Ropi (0 mM, 0.1 mM, 0.5 mM, 1 mM, 2.5 mM, and 5 mM), and the cell viability was detected by cell counting kit-8 (CCK-8) assay at 24, 48, and 72 h after treatment. After the used concentration was confirmed, the next experiments were performed at 48 h after the treatment of cells.

Small interfering RNAs (siRNAs) targeting FOXO3 (si-FOXO3-1, si-FOXO3-2) and miR-126-5p inhibitor (inhi-126), TRAF6 overexpression vector pcDNA3.1 (TRAF6) and corresponding negative controls si-NC, inhi-NC and empty vector pcDNA3.1 NC were obtained from GenePharma Co., Ltd (Shanghai, China). SK-N-SH cells were seeded in the 24-well plates and cultured to 70% confluence. The vectors and inhibitors were transfected into SK-N-SH cells using Lipofectamine 2000 transfection reagent (Invitrogen, Waltham, MA) in accordance with the manufacturer's instructions. Cells were cultured at 37℃ in a humidified 5% CO_2 air. Cells were obtained 48 h later to detect transfection efficiency and then were analyzed by other experiments.

CCK-8 assay The cell viability was detected by the CCK-8 kit (Nanjing Jiancheng Bioengineering Institute, Nanjing, China) according to the manufacturer's instructions. SK-N-SH cells with different treatments were seeded at 5000 cells/well in the 96-well plates. CCK-8 reagent (10 μL/well) was added at 24, 48, and 72 h, respectively. After incubation at 37℃ for 1 h, the optical density (OD) value was measured by a microplate reader (Dojindo Laboratories, Kumamoto, Japan) at 450-nm wavelength.

Measurements of lactate dehydrogenase (LDH), reactive oxygen species (ROS), and superoxide dismutase (SOD) levels LDH release was detected using a kit to determine cytotoxicity according to the manufacturer's instructions (Nanjing Jiancheng Bioengineering Institute, Nanjing, China). SK-N-SH cells with different treatments were collected and then incubated with LDH release reagent for 1 h. After that, the cell supernatant was used to mix with LDH detection reagent, and then it was incubated in the dark at room temperature for 30 min. LDH concentration was quantified by OD value at 490-nm wavelength, using the blank group as a standard.

ROS levels in cells were detected using 2,7-dichlorofluorescein diacetate (DCFDA). After incubation with 50 μM DCFDA for 45 min, the DCFDA medium was removed, and

the cells were washed twice with phosphate-buffered saline (PBS, pH 7.4) solution. Fluorescence intensity of DCFDA was measured using a fluorescence spectrophotometer (Synergy MX, BioTek, Winooski, VT) at an excitation wavelength of 485 nm and an emission wavelength of 538 nm.

SOD levels in cells were measured using the SOD detection kit (Beyotime, Shanghai, China). After cell treatment, the cells were lysed in lysis buffer containing 1% NP-40, 1% sodium deoxycholate, 0.1% sodium dodecyl sulfate, 40 mM β-glycerophosphate, 50 mM sodium fluoride, 2 mM sodium orthovanadate, and a protease inhibitor mixture. Finally, the supernatant was collected to measure SOD activity. Enzyme activity was measured at 420-nm wavelength using a microplate reader (BioTek, Winooski, VT).

TdT-mediated dUTP nick-end labeling (TUNEL) assay TUNEL assay was used to detect cell apoptosis. SK-N-SH cells were seeded in the 12-well plates at a density of 10×10^4 cells/well. Cells were fixed with 4% formaldehyde and were added with the TUNEL reaction mixture according to the manufacturer's instructions, followed by nuclear staining with 4′,6-diamidino-2-phenylindole. All samples were observed under a fluorescence microscope, and three same-sized fields were randomly selected per sample for statistical analysis.

Quantitative real-time polymerase chain reaction (qRT-PCR) The extraction and isolation of total RNA from cells was performed using the TRIzol reagent (Invitrogen, Carlsbad, CA) according to the manufacturer's instructions. RNA was reverse-transcribed using the Power complementary DNA (cDNA) synthesis kit (iNtRON Biotech, Seongnam, Korea) according to the manufacturer's instructions. qRT-PCR analysis was executed using iTaq Universal SYBR Green Supermix (Bio-Rad Laboratories, Inc., Hercules, CA) and an ABI 7500 instrument (Applied Biosystems, Foster City, CA). The relative expression of target genes was normalized according to glyceraldehyde-3-phosphate dehydrogenase or U6 (Zhou *et al*. 2021) and then was quantified by the $2^{-\Delta\Delta Ct}$ method (Livak and Schmittgen 2001). The primer sequences are shown in Table 1.

Western blot (WB) assay Cells were treated with radioimmunoprecipitation assay lysis buffer, and protein was quantified by bicinchoninic acid method. Equal amounts of protein samples were separated on sodium dodecyl sulfate polyacrylamide gel electrophoresis and then were transferred to PVDF membranes. After blocking with 5% skim milk, the cells were incubated with primary antibodies against FOXO3 (1:1000, NBP2-16521, NOVUS, Littleton, CO), TRAF6 (1:5000, ab40675, Abcam, Cambridge, MA), and β-actin (1:1000, ab8227, Abcam, Cambridge, MA) overnight at 4℃. The secondary immunoglobulin G (IgG) antibody (1:2000, ab6721, Abcam, Cambridge, MA) was incubated for 1 h at room temperature. The visualized analysis of Western blots was conducted using the enhanced chemiluminescence system and was quantified using ImageJ software. Normalization was performed using β-actin as a loading control.

Chromatin immunoprecipitation (ChIP) assay ChIP-PCR assay was performed according to the manufacturer's instructions (Millipore, Billerica, MA). SK-N-SH cells were placed in 10-cm dishes and incubated with 1% formaldehyde for 10 min to cross-link proteins with DNA. Next, cells were washed twice with cold PBS containing the protease inhibitor. The washed cells were scraped and resuspended in lysis buffer. The lysate was sonicated and centrifuged to remove cell debris. The volume of chromatin supernatant was divided into three portions. The first portion was used as an input (positive) control, and the remaining two portions were diluted with ChIP dilution buffer containing the protease inhibitor. Chromatin solution was incubated with antibodies FOXO3 (1:1000, NBP2-16521, NOVUS, Littleton, CO) or IgG (1:2000, ab6757, Abcam, Cambridge, MA) and protein A magnetic bead overnight at 4°C while rotating. The attached immune complexes were rinsed to elute. The qRT-PCR was used to analyze enrichment. The information on primer sequences is enlisted in Table 1.

Bioinformatics The JASPAR database (https://jaspar.genereg.net/) (Castro-Mondragon *et al*. 2022) was employed to predict the binding site between FOXO3 and miR-126-5p promoter. TargetScan database (http://www.targetscan.org/vert_71/) (Agarwal *et al*. 2015) and starBase database

Table 1. qPCR primers

	Forward primer (5′-3′)	Reverse primer (5′-3′)
FOXO3	TCACGCACCAATTCTAACGC	CACGGCTTGCTTACTGAAGG
miR-126-5p	GCCGAGCATTATTACTTTTG	CTCAACTGGTGTCGTGGA
TRAF6	ATGCGGCCATAGGTTCTGC	TCCTCAAGATGTCTCAGTTCCAT
U6	GTGCTCGCTTCGGCAGCA	AAAAATATGGAACGCTTCA
GAPDH	CTCAACTACATGGTTTAC	CCAGGGGTCTTACTCCTT
miR-126-5p promoter	CTGTGTGCCCAAGGGAGGGC	TCCCTCCCCATCCTCCCTCCCTG

(http://starbase.sysu.edu.cn/) (Li *et al*. 2014) were used to predict the mRNAs in the downstream of miR-126-5p.

Dual-luciferase reporter assay The wild-type (WT) miR-126-5p promoter sequence binding to FOXO3 and the mutant (MUT) sequence were inserted into the dual-luciferase reporter plasmid to construct the wild-type vector miR-126-WT and the mutant vector miR-126-MUT. The vectors of TRAF6-WT and TRAF6-MUT containing the wild and mutant TRAF6 3′UTR sequences binding to miR-126-5p were constructed in the same way. The plasmids were co-transfected into SK-N-SH cells with miR-126-5p mimic or mimic NC, FOXO3 overexpression vector (FOXO3), or empty vector (NC) using Lipofectamine 3000 (Invitrogen, Carlsbad, CA) according to the manufacturer's instructions. Luciferase activity was determined by a dual-luciferase reporter assay system (Promega, Madison, WI).

Statistical analysis All data were analyzed using SPSS21.0 statistical software (IBM SPSS Statistics, Chicago, IL) and GraphPad Prism 8.0 software (GraphPad Software Inc., San Diego, CA). First, the normality and homogeneity of variance tests were performed, and the result was consistent with normal distribution and homogeneity of variance. The *t* test was used for data comparison between the two groups, and one-way or two-way analysis of variance (ANOVA) was used for data comparison among multiple groups, followed by Tukey's multiple comparisons test. $p < 0.05$ was considered statistically significant.

Results

Ropi induced nerve cell damage and upregulated the expression of FOXO3 SK-N-SH cells were treated with different concentrations of Ropi, and the results showed that the viability of SK-N-SH cells was decreased with the increase of Ropi concentration ($p < 0.05$; Fig. 1*A*). In the subsequent experiments, we uniformly selected 2.5 mM Ropi to treat cells for 48 h. Under the above condition, Ropi decreased cell viability ($p < 0.05$; Fig. 1*A*), induced the production of ROS and LDH, and inhibited the production of SOD ($p < 0.05$; Fig. 1*B–D*), and significantly increased the cell apoptosis rate ($p < 0.01$; Fig. 1*E*). FOXO3 was highly expressed in Ropi-treated cells ($p < 0.01$; Fig. 1*F*, *G*). These results suggested that Ropi induced nerve cell damage and upregulated the expression of FOXO3.

Inhibition of FOXO3 expression improved Ropi-induced nerve cell damage Two siRNAs targeting FOXO3 were designed and transfected into SK-N-SH cells. The expression of FOXO3 was successfully downregulated as detected by qRT-PCR and WB assay ($p < 0.05$; Fig. 2*A*, *B*). Downregulation of FOXO3 expression effectively improved the Ropi-induced nerve cell damage, increased the cell viability ($p < 0.05$; Fig. 2*C*) and SOD ($p < 0.05$; Fig. 2*F*), reduced LDH and ROS levels ($p < 0.05$; Fig. 2*D*, *E*), and inhibited cell apoptosis ($p < 0.05$; Fig. 2*G*). These results indicated that inhibition of FOXO3 expression ameliorated Ropi-induced neuronal injury.

FOXO3 transcriptionally inhibited the expression of miR-126-5p and miR-126-5p targeted the expression of TRAF6 FOXO3, as a transcription factor, can inhibit the expression of miRNA through transcription (Wu *et al*. 2021), and miR-126-5p is poorly expressed in injured nerve cells (Xiao *et al*. 2020). Through the JASPAR database, it was found that FOXO3 had a binding relationship with the miR-126-5p promoter (Fig. 3*A*). ChIP analysis showed that FOXO3 was enriched at the miR-126-5p promoter, and Ropi treatment promoted this enrichment of FOXO3. After inhibiting FOXO3 expression, the enrichment was decreased ($p < 0.01$; Fig. 3*B*). The results of dual-luciferase reporter assay showed that overexpression of FOXO3 vectors significantly inhibited the luciferase activity of WT dual-luciferase reporter vector ($p < 0.01$; Fig. 3*C*). The expression of miR-126-5p was significantly decreased after Ropi treatment and was increased after inhibition of FOXO3 expression ($p < 0.05$; Fig. 3*D*). These results indicated that FOXO3 could bind to the miR-126-5p promoter and inhibit the transcription of miR-126-5p.

Next, the downstream target genes of miR-126-5p were analyzed by the TargetScan database and starBase database, and the intersection was identified (Fig. 3*E*), and then we found that TRAF6 was upregulated in bupivacaine-induced neurotoxicity (Chen and Zhuang 2023). We hypothesized that miR-126-5p might be involved in Ropi-induced neurotoxicity by targeting TRAF6 expression. Dual-luciferase reporter assay showed that the binding of miR-126-5p to the 3′UTR of TRAF6 significantly inhibited the luciferase activity in the system ($p < 0.01$; Fig. 3*C*). The results of qRT-PCR and Western blot assay showed that the mRNA and protein levels of TRAF6 were highly expressed in Ropi-induced cells, and the expression of TRAF6 was decreased after inhibiting the expression of FOXO3 ($p < 0.05$; Fig. 3*D*, *F*), indicating that miR-126-5p could target and inhibit TRAF6 expression.

Inhibition of miR-126-5p expression partially reversed the alleviative effect of FOXO3 knockdown on nerve cell damage The miR-126-5p inhibitor (inhi-126) was transfected into SK-N-SH cells to downregulate the expression of miR-126-5p ($p < 0.01$; Fig. 4*A*) and then a combined experiment with inhi-126 and si-FOXO3-1 was performed to verify the above mechanism. Compared with the cells transfected with si-FOXO3-1 alone, the

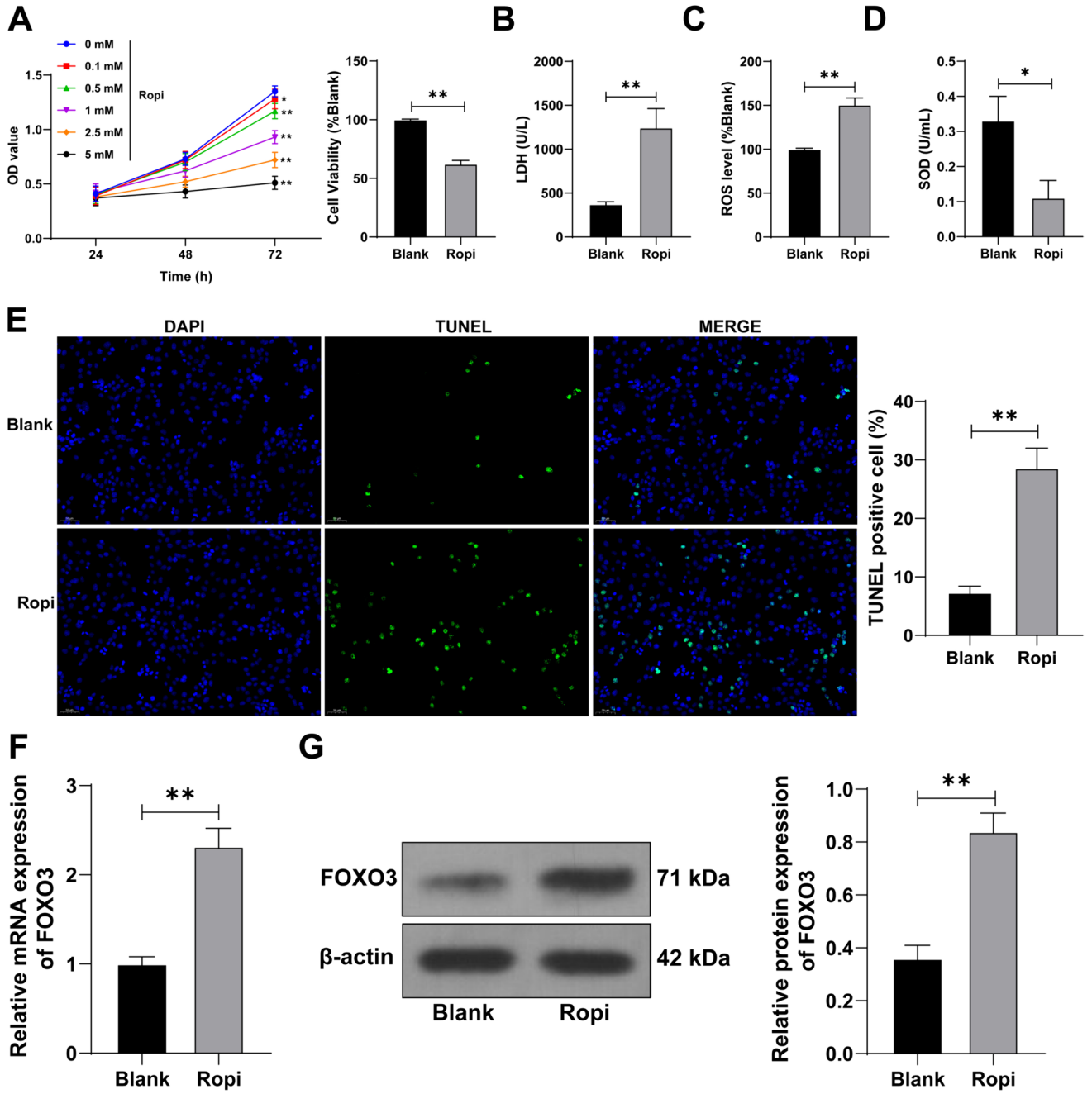

Figure 1. Ropivacaine Ropi induced nerve cell damage and upregulated the expression of FOXO3. SK-N-SH cells were treated with different concentrations of Ropi. (*A*) CCK-8 was used to detect the cell viability at different time points; cells were treated with 2.5 mM Ropi for 48 h. (*B–D*) The contents of LDH, ROS, and SOD in cells were detected respectively. (*E*) TUNEL staining was used to observe cell apoptosis. (*F*, *G*) qRT-PCR and Western blot assay were used to detect the expression of FOXO3. Cell experiments were repeated three times independently. $^{*}p<0.05$, $^{**}p<0.01$. Data (A) (*line graphs*) was analyzed by two-way ANOVA, followed by Tukey's multiple comparisons test. Data (A) (*bar graphs*) and data (B–G) were analyzed by *t* test. Ropi, ropivacaine; LDH, lactate dehydrogenase; ROS, reactive oxygen; SOD, superoxide dismutase.

expression of TRAF6 was increased ($p<0.01$; Fig. 4*A*, *B*), cell viability was reduced ($p<0.01$; Fig. 4*C*), the levels of LDH and ROS were significantly increased, while the level of SOD was decreased ($p<0.05$; Fig. 4*D–F*), and the apoptosis rate was increased ($p<0.01$; Fig. 4*G*) after downregulation of miR-126-5p. These results suggested that inhibition of miR-126-5p expression partially reversed the alleviative effect of FOXO3 knockdown on Ropi-induced nerve cell damage.

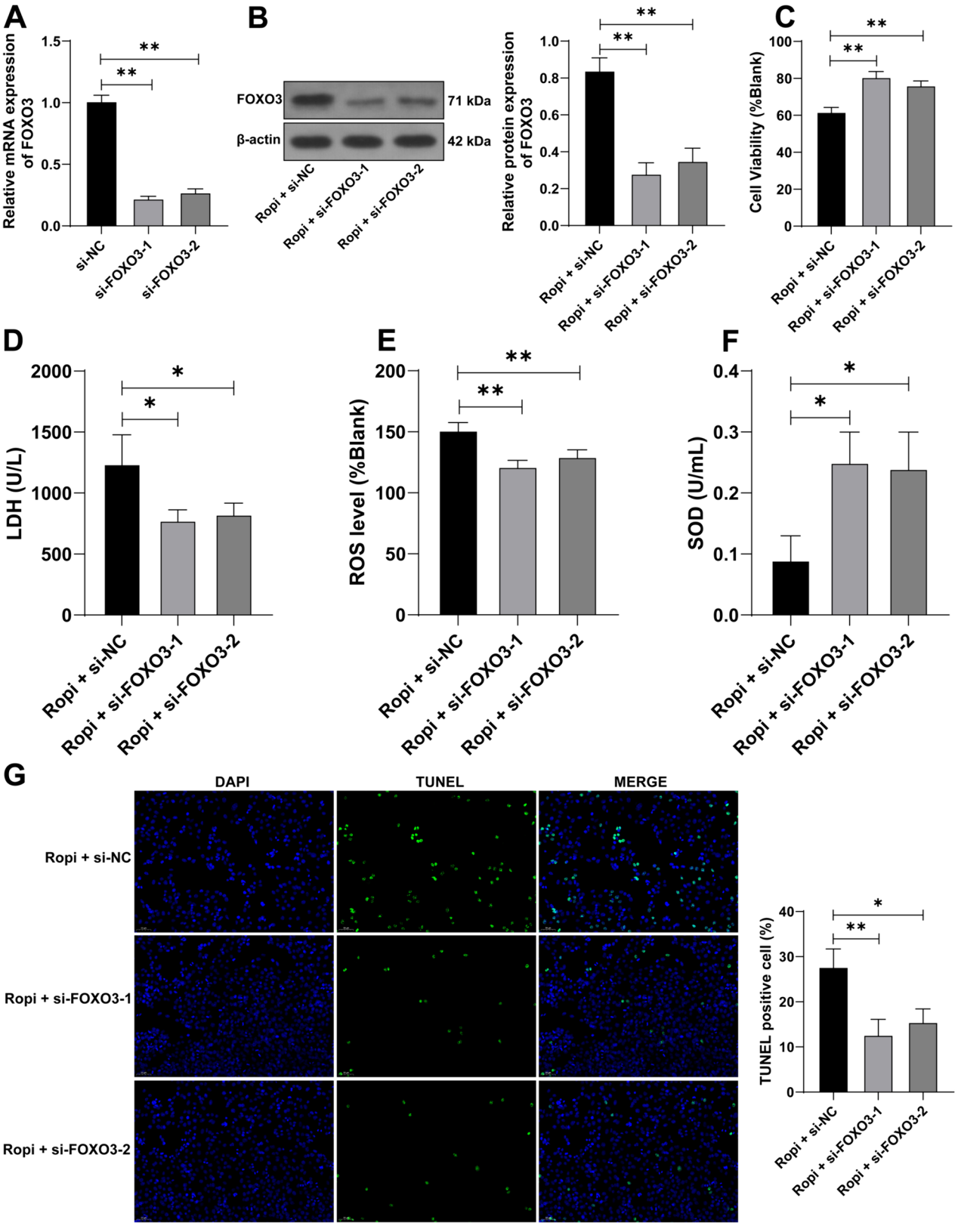

Overexpression of TRAF6 partially reversed the alleviative effect of FOXO3 knockdown on nerve cell damage Finally, we overexpressed TRAF6 in SK-N-SH cells ($p < 0.01$; Fig. 5*A*, *B*) and a combined experiment with

◂**Figure 2.** Inhibition of FOXO3 expression improved Ropi-induced nerve cell damage. Two si-FOXO3 (si-FOXO3-1, si-FOXO3-2) were transfected into SK-N-SH cells, and si-NC was used as control. (*A*) qRT-PCR was used to detect the knockdown efficiency. Transfected cells were treated with 2.5 mM Ropi for 48 h. (*B*) Western blot assay was used to detect FOXO3 expression. (*C*) CCK-8 assay was used to detect cell viability. (*D–F*) The contents of LDH, ROS, and SOD in cells were detected. (*G*) TUNEL staining was used to observe cell apoptosis. Cell experiments were repeated three times independently. $^{*}p < 0.05$, $^{**}p < 0.01$. Data were analyzed by one-way ANOVA, followed by Tukey's multiple comparisons test.

pcDNA3.1-TRAF6 and si-FOXO3-1 was performed. Compared with si-FOXO3-1 transfection alone, the cell viability was reduced ($p < 0.01$; Fig. 5*C*), the levels of LDH and ROS were significantly increased, the level of SOD was decreased ($p < 0.05$; Fig. 5*D–F*), and apoptosis rate was increased ($p < 0.05$; Fig. 5*G*) after overexpression of TRAF6. These results suggested that overexpression of TRAF6 partially reversed the alleviative effect of FOXO3 knockdown on Ropi-induced nerve cell damage.

Discussion

Local anesthetics (LAs) are composed of lipophilic aromatic groups, hydrophilic groups, and amide or ester chains and are divided into aminoamide and aminoester types (Lirk *et al*. 2014). Ropivacaine (Ropi) is a commonly used LA in operations like spinal anesthesia (Contino *et al*. 2021) and cesarean section (Feng *et al*. 2021), but it can cause neurotoxicity in a dose-dependent manner. However, there is a lack of effective adjuvants for the treatment of LA-induced neurotoxicity. In this study, we cultured SK-N-SH cells and treated them with different concentrations of Ropi to explore the mechanism of FOXO3 in Ropi-induced nerve injury. It was found that FOXO3 was highly expressed in Ropi-induced nerve damage cells, and it bound to the miR-126-5p promoter and inhibited its expression to upregulated TRAF6 expression, leading to nerve cell damage.

Ropi causes neuronal dysfunction as manifested by increases in ROS and LDH production (Chen *et al*. 2019). Excessive ROS leads the brain to a vulnerable state and induces mitochondrial dysfunction, leading to nerve cell damage (Fang *et al*. 2017). LDH can be released from acutely damaged neurons, serving as an index of neurotoxicity (Izumi *et al*. 2001). Increasing SOD activity reduces oxidative stress and mitochondrial H_2O_2 levels, and neuronal cell loss (Zhang *et al*. 2021). In our study, it was confirmed that SK-N-SH cell viability decreased with the increase of Ropi concentration. Cells were treated with 2.5 mM Ropi for 48 h to reach the semi-inhibitory concentration. After Ropi treatment, the cell viability and SOD were decreased, while ROS and LDH as well as the apoptosis rate were increased significantly. Importantly, FOXO3 was highly expressed in Ropi-treated cells. FOXO3 is over-activated in sevoflurane-induced neurotoxicity, leading to inappropriate differentiation of nerve stem cells (Zeng *et al*. 2022). Overexpression of FOXO3 can lead to neuronal apoptosis in mouse brain and the death of mouse neuroblastoma neuro-2a cells, worsening neurological outcomes after ischemic cerebral injury (Guo *et al*. 2018). FOXO3 overexpression impairs neurogenesis in mouse embryonic fibroblasts, whereas FOXO3 knockdown promotes the reprogramming efficiency of adult-derived fibroblasts and the functional maturation of resulting induced neuronal cells (Ahlenius *et al*. 2016). FOXO3 is highly expressed in neurons after oxygen–glucose deprivation, leading to neuronal apoptosis and inflammatory response (Deng *et al*. 2020). Our results suggested that inhibition of FOXO3 ameliorated Ropi-induced neuronal injury, indicating that FOXO3 inhibitor may serve as an adjuvant to relieve the neurological side effects caused by LAs.

Furthermore, accumulating data have highlighted that the interaction between FOXO3 and miRNAs regulates the progression of human complex diseases. However, most previous studies reported that miRNAs induce negative regulation of FOXO3 (Li *et al*. 2021; Liu *et al*. 2022), while our study focuses on the less-studied downstream mechanism of FOXO3 involving miRNAs. We found that FOXO3 could bind to the miR-126-5p promoter and inhibit the transcription of miR-126-5p. Previous studies have shown the role of miRNAs in anesthetics-induced neurotoxicity. For example, downregulation of miR-384-5p can inhibit neuronal apoptosis and alleviate ketamine-induced neurotoxicity (Lu *et al*. 2022). Overexpression of miR-128-3p can prevent neuronal apoptosis induced by sevoflurane treatment (Wu *et al*. 2022). In addition, overexpression of miR-126 can improve hippocampal pathological morphology and reduce hippocampal neuronal apoptosis (Lin *et al*. 2020). Increasing the expression level of miR-126 can improve neurological function and promote neurological recovery (Venkat *et al*. 2019). Inhibition of miR-126-3p exacerbated the oxygen and glucose deprivation and reperfusion-induced cell death and reduced cell viability (Xiao *et al*. 2020). Herein, inhibition of miR-126-5p resulted in decreased neuronal cell activity and accelerated apoptosis. Collectively, we revealed for the first time that downregulation of miR-126-5p exacerbates Ropi-induced neuronal damage, and the function of miR-126-5p may relate to hippocampal pathological injury.

TRAF6 is involved in the survival or induction of apoptosis of Schwann cells and major glial cells, affecting nerve cell damage (Yamamoto *et al*. 2021). TRAF6 is upregulated in bupivacaine-induced neurotoxicity, leading to neuronal apoptosis, inhibition of neuronal viability, and production of LDH (Chen and Zhuang 2023). Likewise, TRAF6 is upregulated in isoflurane-induced neurotoxicity, leading to apoptosis and neuroinflammation in the hippocampus (Jiang

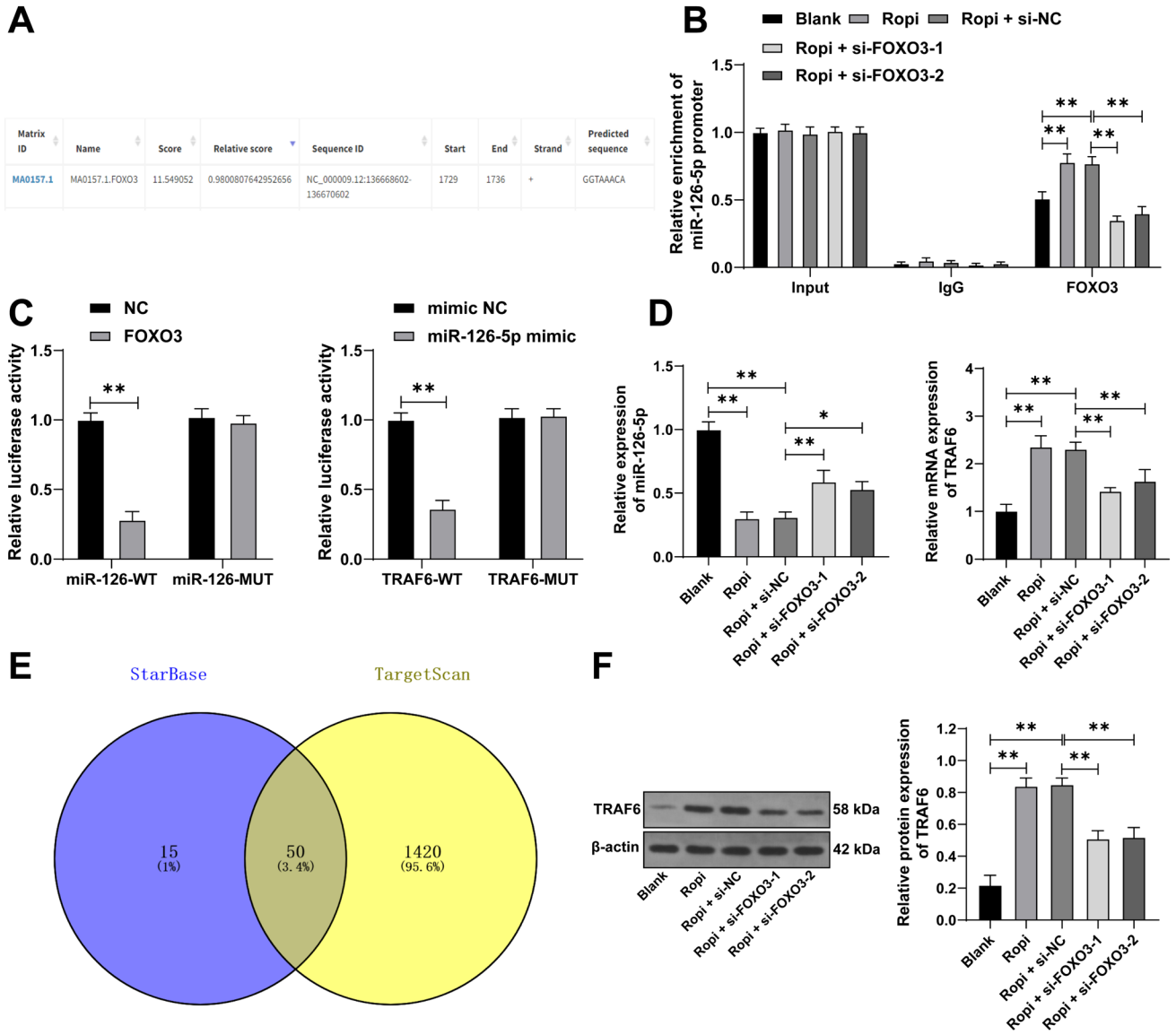

Figure 3. FOXO3 transcriptionally inhibited the expression of miR-126-5p and miR-126-5p targeted the expression of TRAF6. (*A*) The JASPAR database was used to analyze the binding site of FOXO3 and miR-126-5p promoter sequence. (*B*) ChIP assay was used to analyze the enrichment of FOXO3 at the miR-126-5p promoter. (*C*) Dual-luciferase reporter assay was used to detect the binding relationship between FOXO3 and miR-126-5p promoter sequence, as well as miR-126-5p and TRAF6 3′UTR sequence. (*D*) qRT-PCR was used to detect the transcriptional levels of miR-126-5p and TRAF6. (*E*) The downstream target genes of miR-126-5p were analyzed by TargetScan database and starBase database, and the intersection in Venn diagram was identified. (*F*) Western blot assay was used to detect TRAF6 expression. Cell experiments were repeated three times independently. $^{*}p < 0.05$, $^{**}p < 0.01$. Data B and C were analyzed by two-way ANOVA. Data D and F were analyzed by one-way ANOVA, followed by Tukey's multiple comparisons test.

et al. 2021). In our study, miR-126-5p could target the inhibition of TRAF6 expression. We verified that overexpression of TRAF6 reduced cell activity and significantly increased cell apoptosis rate. In summary, TRAF6 inhibition may have the potential to treat neuronal cell damage, which requires further research for confirmation.

Our study still has some limitations. First of all, we only tested Ropi for the neurotoxicity of LAs on nerve cells, and other drugs commonly used in clinical practice have not been tested. Therefore, it is not clear whether the regulatory mechanism of FOXO3/miR-126-5p/TRAF6 is applicable to all local anesthetics-induced neurotoxicity. Secondly, we only carried out the study at the cellular level, and animal experiments are demanded to verify our findings. In the future, we plan to establish animal models to explore whether FOXO3/miR-126-5p/TRAF6 plays the same role in vivo. The role of the FOXO3/miR-126-5p/TRAF6 axis in the neurotoxicity induced by other LAs will be explored.

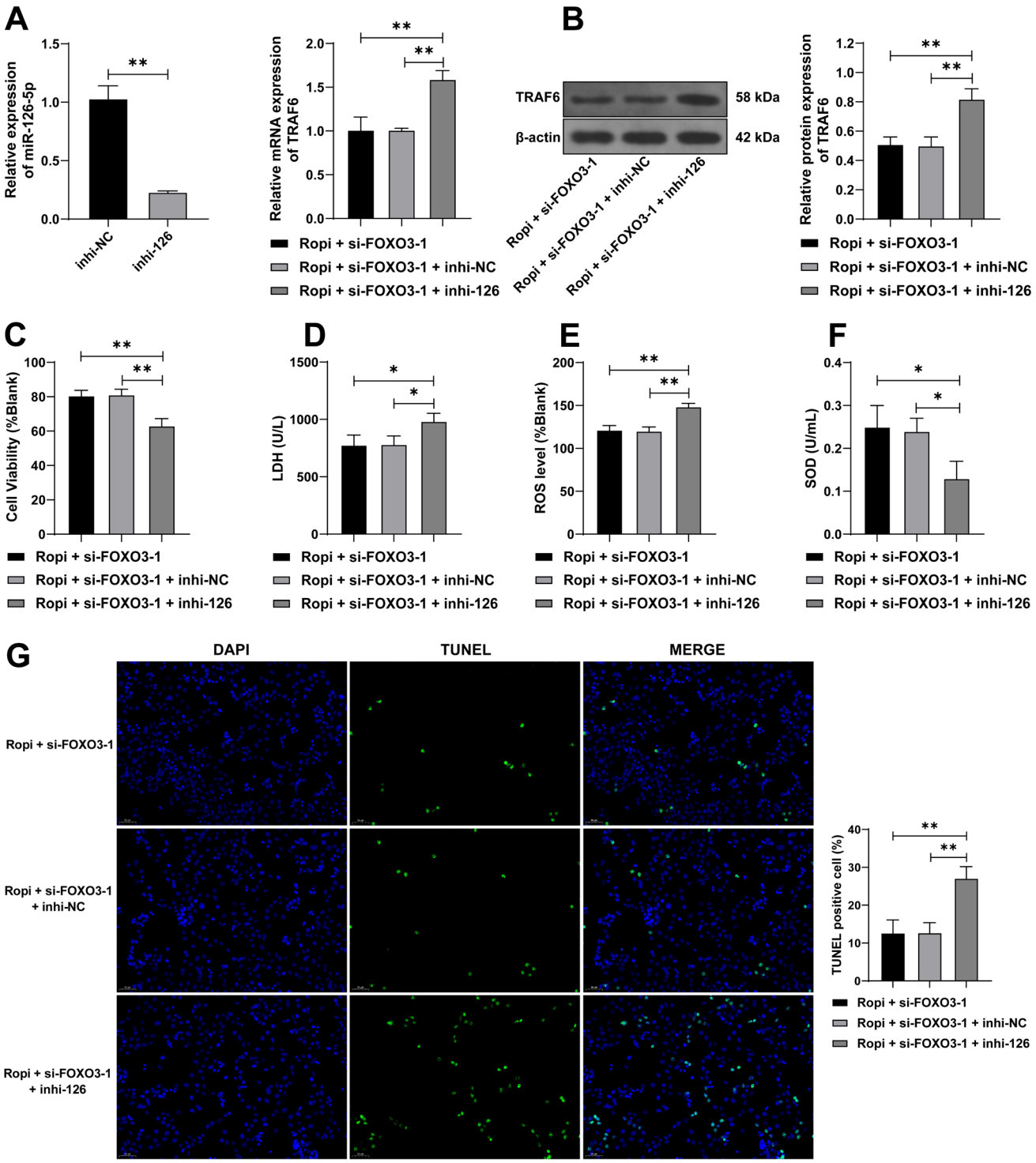

Figure 4. Inhibition of miR-126-5p expression partially reversed the alleviative effect of FOXO3 knockdown on nerve cell damage. miR-126-5p inhibitor (inhi-126) was transfected into SK-N-SH cells and a combined experiment was performed with si-FOXO3-1, with inhi-NC as the control. Transfected cells were treated with 2.5 mM Ropi for 48 h. (*A*) qRT-PCR was used to detect the transcription of miR-126-5p and TRAF6. (*B*) Western blot assay was used to detect TRAF6 expression. (*C*) CCK-8 was used to detect cell viability. (*D–F*) The contents of LDH, ROS, and SOD in cells were detected, respectively. (*G*) TUNEL staining was used to observe cell apoptosis. Cell experiments were repeated three times independently. $*p < 0.05$, $**p < 0.01$. Data (A) (*left*) were analyzed by *t* test. Data (A) (*right*) and data (B–G) were analyzed by one-way ANOVA, followed by Tukey's multiple comparisons test.

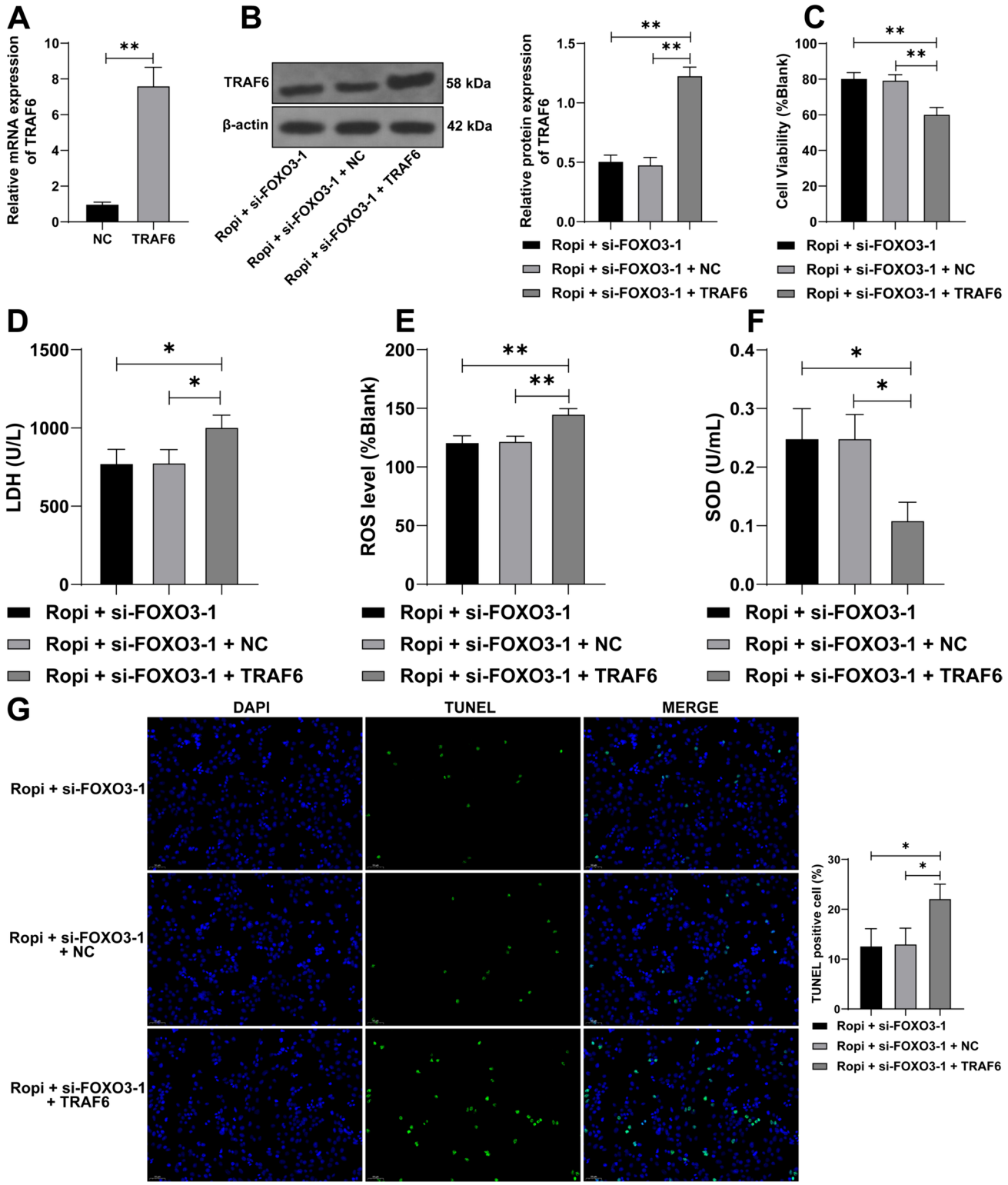

Figure 5. Overexpression of TRAF6 partially reversed the alleviative effect of FOXO3 knockdown on nerve cell damage. TRAF6 overexpression vector pcDNA3.1-TRAF6 (TRAF6) was transfected into SK-N-SH cells and a combined experiment with si-FOXO3-1 was performed, with empty vector pcDNA3.1 (NC) as the control. Transfected cells were treated with 2.5 mM Ropi for 48 h. (*A*, *B*) qRT-PCR and Western blot assay were used to detect the expression of TRAF6. (*C*) CCK-8 was used to detect cell viability. (*D–F*) The contents of LDH, ROS, and SOD in cells were detected, respectively. (*G*) TUNEL staining was used to observe cell apoptosis. Cell experiments were repeated three times independently, $*p<0.05$, $**p<0.01$. Data (A) were analyzed by *t* test. Data (B–G) were analyzed by one-way ANOVA, followed by Tukey's multiple comparisons test.

To sum up, we found that FOXO3 can transcriptionally inhibit the expression of miR-126-5p and then repress TRAF6 to aggravate Ropi-induced nerve damage. Our results provide a theoretical basis for the remission of the neurotoxicity caused by LAs.

Declarations

Conflict of interest The authors declare no competing interests.

References

Agarwal V, Bell GW, Nam JW, Bartel DP (2015) Predicting effective microRNA target sites in mammalian mRNAs. Elife 4:e05005

Ahlenius H, Chanda S, Webb AE, Yousif I, Karmazin J, Prusiner SB, Brunet A, Sudhof TC, Wernig M (2016) FoxO3 regulates neuronal reprogramming of cells from postnatal and aging mice. Proc Natl Acad Sci U S A 113:8514–8519

Barletta M, Reed R (2019) Local anesthetics: pharmacology and special preparations. Vet Clin North Am Small Anim Pract 49:1109–1125

Bhargava S, Patil V, Mahalingam K, Somasundaram K (2017) Elucidation of the genetic and epigenetic landscape alterations in RNA binding proteins in glioblastoma. Oncotarget 8:16650–16668

Cao G, Lin M, Gu W, Su Z, Duan Y, Song W, Liu H, Zhang F (2023) The rules and regulatory mechanisms of FOXO3 on inflammation, metabolism, cell death and aging in hosts. Life Sci 328:121877

Castro-Mondragon JA, Riudavets-Puig R, Rauluseviciute I, Lemma RB, Turchi L, Blanc-Mathieu R, Lucas J, Boddie P, Khan A, Manosalva Perez N, Fornes O, Leung TY, Aguirre A, Hammal F, Schmelter D, Baranasic D, Ballester B, Sandelin A, Lenhard B, Vandepoele K, Wasserman WW, Parcy F, Mathelier A (2022) JASPAR 2022: the 9th release of the open-access database of transcription factor binding profiles. Nucleic Acids Res 50:D165–D173

Chen L, Zhuang K (2023) Kaempferol counteracts bupivacaine-induced neurotoxicity in mouse dorsal root ganglia neurons by regulating TRAF6-dependent NF-kappaB signaling. Kaohsiung J Med Sci 39:710–717

Chen Y, Gao X, Pei H (2022) miRNA-384-3p alleviates sevoflurane-induced nerve injury by inhibiting Aak1 kinase in neonatal rats. Brain Behav 12:e2556

Chen Y, Yan L, Zhang Y, Yang X (2019) The role of DRP1 in ropivacaine-induced mitochondrial dysfunction and neurotoxicity. Artif Cells Nanomed Biotechnol 47:1788–1796

Contino V, Abrams JH, Arumugam S, Sinha SK, Vellanky SS, Cremins MS, McCann GP (2021) Spinal anesthesia using ropivacaine leads to earlier ambulation after total hip arthroplasty. Orthopedics 44:e343–e346

Deng Y, Ma G, Gao F, Sun X, Liu L, Mo D, Ma N, Song L, Huo X, He H, Miao Z (2020) SOX9 Knockdown-mediated FOXO3 down-regulation confers neuroprotection against ischemic brain injury. Front Cell Dev Biol 8:555175

Diener C, Keller A, Meese E (2022) Emerging concepts of miRNA therapeutics: from cells to clinic. Trends Genet 38:613–626

Fang C, Gu L, Smerin D, Mao S, Xiong X (2017) The interrelation between reactive oxygen species and autophagy in neurological disorders. Oxid Med Cell Longev 2017:8495160

Feng G, Wang Y, Feng J, Luo X, Li C, Yao S (2021) The relationship between core temperature and perioperative shivering during caesarean section under intrathecal anesthesia with bupivacaine and ropivacaine: a randomized controlled study. J Anesth 35:889–895

Guo D, Ma J, Li T, Yan L (2018) Up-regulation of miR-122 protects against neuronal cell death in ischemic stroke through the heat shock protein 70-dependent NF-kappaB pathway by targeting FOXO3. Exp Cell Res 369:34–42

Hampl K, Steinfeldt T, Wulf H (2014) Spinal anesthesia revisited: toxicity of new and old drugs and compounds. Curr Opin Anaesthesiol 27:549–555

Izumi Y, Izumi M, Benz AM, Zorumski CF (2001) Lactate dehydrogenase release is facilitated by brief sonication of rat hippocampal slices and isolated retinas following acute neuronal damage. J Neurosci Methods 108:49–55

Jiang T, Xu S, Shen Y, Xu Y, Li Y (2021) Genistein attenuates isoflurane-induced neuroinflammation by inhibiting TLR4-mediated microglial-polarization in vivo and in vitro. J Inflamm Res 14:2587–2600

Li JH, Liu S, Zhou H, Qu LH, Yang JH (2014) starBase v2.0: decoding miRNA-ceRNA, miRNA-ncRNA and protein-RNA interaction networks from large-scale CLIP-Seq data. Nucleic Acids Res 42:D92-97

Li W, Zhu Q, Xu X, Hu X (2021) MiR-27a-3p suppresses cerebral ischemia-reperfusion injury by targeting FOXO1. Aging (Albany NY) 13:11727–11737

Lin J, Li G, Xu C, Lu H, Zhang C, Pang Z, Liu Z (2020) Monocyte chemotactic protein 1-induced protein 1 is highly expressed in inflammatory bowel disease and negatively regulates neutrophil activities. Mediators Inflamm 2020:8812020

Lirk P, Picardi S, Hollmann MW (2014) Local anaesthetics: 10 essentials. Eur J Anaesthesiol 31:575–585

Liu Y, Dong ZJ, Song JW, Liang LR, Sun LL, Liu XY, Miao R, Xu YL, Li XT, Zhang MW, Zhang ZZ, Zhong JC (2022) MicroRNA-122-5p promotes renal fibrosis and injury in spontaneously hypertensive rats by targeting FOXO3. Exp Cell Res 411:113017

Livak KJ, Schmittgen TD (2001) Analysis of relative gene expression data using real-time quantitative PCR and the 2(-Delta Delta C(T)) Method. Methods 25:402–408

Lu H, Chen Y, Wang X, Yang Y, Ding M, Qiu F (2022) Circular RNA HIPK3 aggravates sepsis-induced acute kidney injury via modulating the microRNA-338/forkhead box A1 axis. Bioengineered 13:4798–4809

Lu Y, Cao DL, Jiang BC, Yang T, Gao YJ (2015) MicroRNA-146a-5p attenuates neuropathic pain via suppressing TRAF6 signaling in the spinal cord. Brain Behav Immun 49:119–129

Mao X, Wu Y, Xu W (2023) miR-126-5p expression in the plasma of patients with sepsis-induced acute lung injury and its correlation with inflammation and immune function. Clin Respir J 17:629–637

Pan J, Qu M, Li Y, Wang L, Zhang L, Wang Y, Tang Y, Tian HL, Zhang Z, Yang GY (2020) MicroRNA-126-3p/-5p overexpression attenuates blood-brain barrier disruption in a mouse model of middle cerebral artery occlusion. Stroke 51:619–627

Park HH (2018) Structure of TRAF family: current understanding of receptor recognition. Front Immunol 9:1999

Qin Z, Zhu G, Luo H, Deng Y (2022) Regulation of FOXO3 on neuronal ferroptosis after intracerebral hemorrhage via modulating NOX4 transcription. Eur Surg Res. https://doi.org/10.1159/000527617

Roux PP, Barker PA (2002) Neurotrophin signaling through the p75 neurotrophin receptor. Prog Neurobiol 67:203–233

Santo EE, Paik J (2018) FOXO in neural cells and diseases of the nervous system. Curr Top Dev Biol 127:105–118

Venkat P, Cui C, Chopp M, Zacharek A, Wang F, Landschoot-Ward J, Shen Y, Chen J (2019) MiR-126 mediates brain endothelial cell exosome treatment-induced neurorestorative effects after stroke in type 2 diabetes mellitus mice. Stroke 50:2865–2874

Wang R, Liu P, Li F, Qiao H (2023) Dexmedetomidine protects against ropivacaine-induced neuronal pyroptosis via the Nrf2/HO-1 pathway. J Toxicol Sci 48:139–148

Wu D, Lee YG, Liu HC, Yuan RY, Chiou HY, Hung CH, Hu CJ (2013) Identification of TLR downstream pathways in stroke patients. Clin Biochem 46:1058–1064

Wu J, Man D, Shi D, Wu W, Wang S, Wang K, Li Y, Yang L, Bian X, Wang Q, Li L (2022) Intermittent fasting alleviates risk markers in a murine model of ulcerative colitis by modulating the gut microbiome and metabolome. Nutrients 14:5311

Wu X, Dai M, Li J, Cai J, Zuo Z, Ni S, Zhang Q, Zhou Z (2021) m(6)A demethylase ALKBH5 inhibits cell proliferation and the metastasis of colorectal cancer by regulating the FOXO3/miR-21/SPRY2 axis. Am J Transl Res 13:11209–11222

Xiao ZH, Wang L, Gan P, He J, Yan BC, Ding LD (2020) Dynamic changes in miR-126 expression in the hippocampus and penumbra following experimental transient global and focal cerebral ischemia-reperfusion. Neurochem Res 45:1107–1119

Xu W, Li X, Chen L, Luo X, Shen S, Wang J (2022) Dexmedetomidine pretreatment alleviates ropivacaine-induced neurotoxicity via the miR-10b-5p/BDNF axis. BMC Anesthesiol 22:304

Xue Y, Xu T, Jiang W (2020) Dexmedetomidine protects PC12 cells from ropivacaine injury through miR-381/LRRC4 /SDF-1/CXCR4 signaling pathway. Regen Ther 14:322–329

Yamamoto M, Gohda J, Akiyama T, Inoue JI (2021) TNF receptor-associated factor 6 (TRAF6) plays crucial roles in multiple biological systems through polyubiquitination-mediated NF-kappaB activation. Proc Jpn Acad Ser B Phys Biol Sci 97:145–160

Yan D, Yang Y, Lang J, Wang X, Huang Y, Meng J, Wu J, Zeng X, Li H, Ma H, Gao L (2023) SIRT1/FOXO3-mediated autophagy signaling involved in manganese-induced neuroinflammation in microglia. Ecotoxicol Environ Saf 256:114872

Yao Y, Wang X, Gao J (2020) LncRNA KCNQ1OT1 sponges miR-206 to ameliorate neural injury induced by anesthesia via up-regulating BDNF. Drug Des Devel Ther 14:4789–4800

Ye Q, Li H, Xu B, He Z, Yan X (2023) Butyrate improves porcine endometrial epithelial cell receptivity via enhancing acetylation of histone H3K9. Mol Nutr Food Res 67:e2200703

Zeng Y, Zhang X, Li F, Wang Y, Wei M (2022) AFF3 is a novel prognostic biomarker and a potential target for immunotherapy in gastric cancer. J Clin Lab Anal 36:e24437

Zhang H, Wang R (2023) TWEAK knockdown alleviates post-cardiac arrest brain injury via the p38 MAPK/NF-kappaB pathway. Discov Med 35:503–516

Zhang W, Hong J, Zhang H, Zheng W, Yang Y (2021) Astrocyte-derived exosomes protect hippocampal neurons after traumatic brain injury by suppressing mitochondrial oxidative stress and apoptosis. Aging (Albany NY) 13:21642–21658

Zhou J, Liu J, Gao Y, Shen L, Li S, Chen S (2021) miRNA-based potential biomarkers and new molecular insights in ulcerative colitis. Front Pharmacol 12:707776